Hybrid Quantum Device Based on *NV* Centers in Diamond Nanomechanical Resonators Plus Superconducting Waveguide Cavities

Peng-Bo Li,[1] Yong-Chun Liu,[2] S.-Y. Gao,[1] Ze-Liang Xiang,[3] Peter Rabl,[3] Yun-Feng Xiao,[2] and Fu-Li Li[1]

[1]*Department of Applied Physics, Institute of Quantum Optics and Quantum Information, Xi'an Jiaotong University, Xi'an 710049, China*

[2]*State Key Laboratory for Mesoscopic Physics, School of Physics, Peking University; Collaborative Innovation Center of Quantum Matter, Beijing 100871, China*

[3]*Institute of Atomic and Subatomic Physics, TU Wien, Stadionallee 2, 1020 Wien, Austria*

(Received 25 August 2014; revised manuscript received 4 August 2015; published 8 October 2015)

We propose and analyze a hybrid device by integrating a microscale diamond beam with a single built-in nitrogen-vacancy (*NV*) center spin to a superconducting coplanar waveguide (CPW) cavity. We find that under an ac electric field the quantized motion of the diamond beam can strongly couple to the single cavity photons via a dielectric interaction. Together with the strong spin-motion interaction via a large magnetic-field gradient, it provides a hybrid quantum device where the diamond resonator can strongly couple both to the single microwave-cavity photons and to the single *NV* center spin. This enables coherent information transfer and effective coupling between the *NV* spin and the CPW cavity via mechanically dark polaritons. This hybrid spin-electromechanical device, with tunable couplings by external fields, offers a realistic platform for implementing quantum information with single *NV* spins, diamond mechanical resonators, and single microwave photons.

DOI: 10.1103/PhysRevApplied.4.044003

I. INTRODUCTION

Hybrid quantum architectures (for a review, see Ref. [1]) take the advantages and strengths of different components, involving degrees of freedom of completely different nature, which are promising for developing quantum technologies and discovering rich physics. Furthermore, the construction of hybrid quantum devices can benefit greatly from the progress achieved so far in the fields of atomic physics, quantum optics, condensed-matter physics, and nanoscience. A growing interest is emerging for exploring hybrid quantum architectures that could find applications in implementing quantum technologies. Prominent examples include superconducting waveguide cavities or mechanical resonators coupled to cold atoms [2–7], polar molecules [8–10], and quantum dots [11–15], as well as other solid-state spin systems [16–36].

A key challenge in the field of hybrid quantum systems is the realization of a controlled interface between a superconducting circuit and a *single* solid-state spin qubit. It would allow the realization of long-lived quantum memories for superconducting qubits, without the big problem of inhomogeneous broadening encountered in spin ensembles [37]. However, the direct magnetic coupling between a single spin and a single microwave photon is typically only a few hertz [2], much smaller than the relevant decoherence rates. To overcome this problem, it has been proposed to enhance this coupling via an intermediate persistent current loop [21,22], but the decoherence rates of such small superconducting loops are still unknown and will to a large extent compensate the achievable increase in coupling strength.

In this work, we propose and analyze a practical design for a coherent quantum interface between a single spin qubit and a microwave resonator, which makes use of the recent advances in the fabrication of single-crystal diamond nanoresonators. Over the past years, mechanical resonators made out of diamond have received considerable attention for the study of fundamental physics, as well as for applications in quantum science and technology [25,38–44]. Diamond, in addition to possessing desirable mechanical and optical properties, can host defect color centers [45], whose highly coherent electronic spins are particularly useful for quantum-information processing at room temperature. Single-crystal diamond cantilevers with exceptional quality factors exceeding one million have been demonstrated in a recent experiment [38]. Moreover, hybrid quantum systems, consisting of single-crystal diamond cantilevers with embedded *NV* center spins, have been realized in recent experiments [39,40]. Such on-chip devices, enabling direct coupling between mechanical and spin degrees of freedom, can be used as key components for hybrid quantum systems.

In the setup investigated in this work, a doubly clamped diamond microbeam with a single built-in *NV* center is placed in the near field of a coplanar waveguide (CPW) cavity (see Fig. 1). Compared to previously considered capacitive coupling schemes [46] usually employed in cavity electromechanics [47–49], we here consider the case where the coupling between the quantized motion of the diamond beam and the microwave-cavity photons results from the dielectric interaction—a fundamental

mechanism that any polarizable body placed in an inhomogeneous electric field will experience a dielectric force. This dielectric coupling is employed in the classical regime for the on-chip actuation of thin mechanical beams [50] and is scalable to large arrays of diamond mechanical resonators. For the present purpose of a quantum interface, it is important that this dielectric coupling is fully controlled by a tunable driving field but opposed to the capacitive coupling [47–49]; it results in large photon-phonon interactions without driving the cavity mode itself. When combined with a magnetic spin-phonon interaction in the presence of a strong magnetic-field gradient [51], a tunable coupling for exchanging a quantum state between the single spin memory and the superconducting microwave cavity can be implemented. We show that under realistic conditions the resulting effective interactions between a single spin qubit and a single microwave photon can exceed 10 kHz, roughly 3 orders of magnitude stronger than the direct coupling. The state transfer can further be optimized by employing a resonant state transfer scheme via mechanically dark polaritons, and we discuss the expected transfer fidelities for different parameters.

II. DESCRIPTION OF THE DEVICE

A. The setup

As shown in Figs. 1(a) and 1(b), a doubly clamped microscale diamond beam embedding a single spin-1 NV center is positioned along the z axis at a distance x_0 from the gap of the CPW cavity surface. The configuration shown in Figs. 1(c) and 1(d) is somewhat equivalent to that of Figs. 1(a) and 1(b). Through small tip electrodes [52,53], a strong ac electric field $\vec{E}_p(t)$ (with frequency ω_p and amplitude E_p) is applied to the diamond beam, which

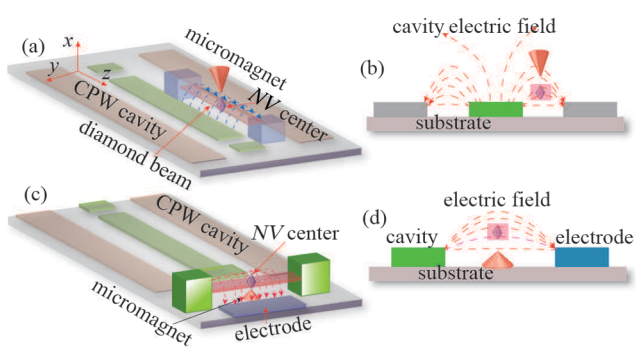

FIG. 1. Schematic of a hybrid device for coupling a doubly clamped diamond microbeam with a single, well-controlled embedded NV center spin to the CPW cavity field. (a) Top view of the configuration of the diamond beam positioned near $z_0 \sim L$ above the gap of the CPW cavity. (b) Side view of the device shown in (a). (c) Top view of a different device where the beam couples to the electric field between the central conductor stripe of the CPW cavity and an external electrode. (d) Side view of the device shown in (c).

induces a large macroscopic electric-dipole moment. The diamond beam of length l has a circular cross section of radius r ($r \ll l$). As the beam vibrates, x_0 changes by the beam's effective transverse displacement, and restricted to the lowest vibrational mode it can be modeled as a harmonic oscillator with frequency ω_m and bosonic mode operator $\hat{b}$. For a thin beam, the resonance frequency ω_m can be calculated by the Euler-Bernoulli theory, i.e., $\omega_m = k_0^2\sqrt{EI/\rho A}$ [54], where $k_0 = 4.73/l$ is the wave number of the fundamental mode, E is the Young's modulus, I is the moment of inertia, ρ is the density of diamond, and A is the cross-section area.

The CPW cavity consisting of a central conductor stripe plus two ground planes is fabricated on a dielectric substrate which supports quasi-TEM microwave fields strongly confined near the gaps between the conductor and the ground planes (Fig. 2). For a CPW cavity of stripline length L and electrode distance d (with effective cavity volume $V_c \sim \pi d^2 L$), the single-mode electric-field operator of the CPW cavity (with frequency ω_c) can be written as [54] $\hat{\vec{E}}_c(\vec{r},t) = \mathcal{E}_0\vec{e}_{\rm tr}(x,y)(\hat{a}e^{-i\omega_c t} + \hat{a}^\dagger e^{i\omega_c t})\cos(\pi z/L)$, where $\mathcal{E}_0 = \sqrt{\hbar\omega_c/\epsilon_0 V_c}$ is the field amplitude, $\vec{e}_{\rm tr}(x,y)$ the dimensionless transverse mode function (see the simulations in Fig. 2), and $\hat{a}$ the destruction operator for the microwave-cavity photons. Then, the free Hamiltonian for the CPW cavity field reads $\hat{H}_c = \hbar\omega_c(\hat{a}^\dagger\hat{a} + \frac{1}{2})$.

B. Dielectric interaction

We first describe the coupling between the diamond beam and the localized electric field of the CPW cavity.

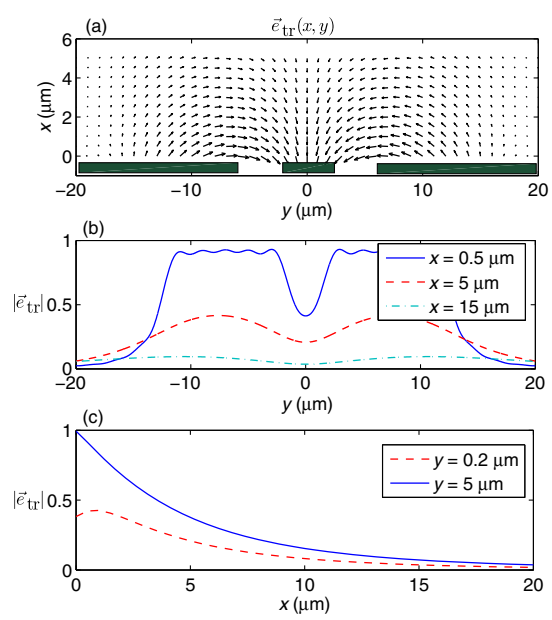

FIG. 2. (a) Distribution of the transverse electric field (per photon) above the CPW cavity. (b),(c) The electric field (per photon) at various positions above the surface of the CPW cavity.

Generally, the electrostatic interaction between a dielectric object and electric fields can be described by $\hat{H}_{\rm pol} = -\frac{1}{2}\int_V \vec{P}(\vec{r})\cdot\vec{E}(\vec{r})d\vec{r}$, where $\vec{P}(\vec{r})$ is the polarization induced by the electric field $\vec{E}(\vec{r})$. In the linear response regime, the polarization field responds linearly to the electric field, such that $\vec{P} = \alpha\vec{E}$, where α is the polarizability tensor, which depends on the symmetry of the diamond beam and its relative orientation with the cavity. The diamond beam is assumed to be placed in parallel with the gap of the cavity, i.e., along the z direction as shown in Fig. 1(a). The total electric field affected by the diamond beam is a transverse field, which can be written as $\vec{E}_\perp(\vec{r},t) = \vec{E}_p(t) + \hat{\vec{E}}_c(\vec{r},t)$.

Considering the case where the dimension of the diamond beam is much smaller than the wavelength of the field, its dielectric response is well approximated by a point dipole, and the components of the polarizability tensor can be approximated by those induced by a uniform electric field. The polarization responds linearly to the electric field, approximating to $\vec{P}(\vec{r}) = \alpha_\perp\vec{E}_\perp + \alpha_z\vec{E}_z$, $\alpha_\perp = \epsilon_0(\epsilon_r - 1)/[1 + N_\perp(\epsilon_r - 1)]$, $\alpha_z = \epsilon_0(\epsilon_r - 1)/[1 + N_z(\epsilon_r - 1)]$ for a dielectric microbeam [55], where ϵ_0 is the free space permittivity, $\epsilon_r = \epsilon/\epsilon_0$, $N_z = \frac{1-e^2}{2e^3}(\ln(1+e)/(1-e) - 2e)$, $N_\perp = \frac{1}{2}(1 - N_z)$, and $e = \sqrt{1 - r^2/l^2}$. Here the transversal and longitudinal directions are defined by the coordinate axes as shown in Fig. 1(a).

As the beam vibrates, the cavity electric field affected by the beam is modulated by the vibration. We first derive the interaction between the CPW cavity field and the diamond beam depicted in Figs. 1(a) and 1(b). Expanding the cavity-field operator around the position of the beam up to first order in the transverse displacement operator $\hat{q}_x$, we obtain [54] $\hat{H}_{\rm pol} = -V\alpha_\perp\vec{E}_p\cdot\partial_x\vec{E}_c(\vec{r},t)\hat{q}_x$, with V the volume of the diamond beam. By assuming $\Delta = \omega_p - \omega_c \ll \omega_p, \omega_c$ and neglecting all rapidly oscillating terms, we obtain the linear photon-phonon coupling [54]

$$\hat{H}_{\rm pol} = \hbar g(\hat{a}e^{i\Delta t} + \hat{a}^\dagger e^{-i\Delta t})(\hat{b}e^{-i\omega_m t} + \hat{b}^\dagger e^{i\omega_m t}). \quad (1)$$

Here

$$g = -\frac{1}{\hbar}V\alpha_\perp\mathcal{E}_0\vec{E}_p\cdot[\partial_x\vec{e}_{\rm tr}(x,y)]_{(x_0,y_0)}\sqrt{\frac{\hbar}{2m\omega_m}}, \quad (2)$$

where m is the effective mass of the mechanical resonator. This coupling strength is proportional to the classic electric-field amplitude and the cavity-field gradient along the transverse direction. It can be greatly enhanced, since the classical electric-field amplitude E_p can be very large for strong enough fields, and the high concentration of cavity-field energy near the surface of the CPW cavity results in a dramatic enhancement of the field per photon $\mathcal{E}_0$ and a large field gradient.

Now we consider the coupling between the CPW cavity and the diamond beam as depicted in Figs. 1(c) and 1(d). In this device, the beam couples to the electric field between the central conductor stripe of the CPW cavity and an external electrode. Therefore, we can use the voltage distribution of the cavity $u(z) = u_0\cos(\pi z/L)(\hat{a}^\dagger + \hat{a})$, with $u_0 = \sqrt{\hbar\omega_c/C}$ and C the total capacitance of the cavity. The electric field from the electrodes is approximated as $|E_c| \sim u_0\zeta/h$, and $|\partial E_c/\partial x| \sim u_0\zeta/h^2$, where h is the height of the beam above the substrate and ζ is a dimensionless constant of order unity set by the electrode geometry [6]. Then the coupling between the beam and the cavity in the interaction picture can be approximated as

$$\begin{aligned}\hat{H}_{\rm pol} &= -V\alpha_\perp E_p\frac{\partial E_c}{\partial x}\hat{q}_x(\hat{a}^\dagger e^{-i\Delta t} + \hat{a}e^{i\Delta t})\\ &= \hbar g(\hat{a}e^{i\Delta t} + \hat{a}^\dagger e^{-i\Delta t})(\hat{b}e^{-i\omega_m t} + \hat{b}^\dagger e^{i\omega_m t}) \quad (3)\end{aligned}$$

with

$$g = -V\alpha_\perp E_p\frac{u_0\zeta}{h^2}\sqrt{\frac{1}{2m\hbar\omega_m}}. \quad (4)$$

The linear coupling between the CPW cavity field and the vibrational mode of the beam is analogous to the effect of radiation pressure on a moving mirror of an optical cavity [56,57] or the capacitive coupling between the motion of a mechanical resonator and an electrical circuit [47–49]. However, different from the previous studies in optomechanics with linear optomechanical coupling, here the coupling is at the *single-photon and -phonon level*. If the detuning is chosen as $\Delta = \omega_p - \omega_c \sim \omega_m \gg g$, then under the rotating-wave approximation we can obtain the beam-splitter Hamiltonian

$$\mathcal{H}_1 = \hbar\Delta\hat{a}^\dagger\hat{a} + \hbar\omega_m\hat{b}^\dagger\hat{b} + \hbar g\hat{a}^\dagger\hat{b} + \hbar g\hat{a}\hat{b}^\dagger. \quad (5)$$

C. Cooling of the vibration mode

We now discuss ground-state cooling of the vibration mode of the diamond beam through the cavity-assisted sideband cooling approach in the resolved sideband regime [58–60], where $\omega_m > \kappa$, with κ being the cavity decay rate. For the mechanical mode of frequency $\omega_m/2\pi \sim 320$ kHz, assuming an environmental temperature $T \sim 20$ mK, the thermal phonon number is about $n_{\rm th} \sim 10^3$. Thus, additional cooling of the vibration mode is needed.

Taking the dissipations of mechanical motion and cavity photons into consideration, the electromechanical system is governed by the quantum master equation

$$\frac{d\hat{\rho}}{dt} = -\frac{i}{\hbar}[\mathcal{H}_1, \hat{\rho}] + \kappa\mathcal{D}[\hat{a}]\hat{\rho} + n_{\rm th}\gamma_m\mathcal{D}[\hat{b}^\dagger] + (n_{\rm th}+1)\gamma_m\mathcal{D}[\hat{b}], \tag{6}$$

with κ the cavity photon loss rate, γ_m the mechanical damping rate of the beam due to clamping, $n_{\rm th} = (e^{\hbar\omega_m/k_BT} - 1)^{-1}$ the thermal phonon number at the environment temperature T, and $\mathcal{D}[\hat{o}]\hat{\rho} = \hat{o}\,\hat{\rho}\,\hat{o}^\dagger - \frac{1}{2}\hat{o}^\dagger\hat{o}\,\hat{\rho} - \frac{1}{2}\hat{\rho}\hat{o}^\dagger\hat{o}$ for a given operator $\hat{o}$. We focus on the resolved sideband regime $\omega_m \gg \kappa$ and set $\Delta = \omega_m$, in which the beam-splitter interaction is on resonance. To realize cooling, the cooperativity $4g^2/\gamma\kappa \gg 1$ and the dynamical stability condition from the Routh-Hurwitz criterion $2g < \omega_m$ should be satisfied.

To calculate the mean phonon number $n_m = \langle\hat{b}^\dagger\hat{b}\rangle$, we need to determine the mean values of all the second-order moments $\langle\hat{a}^\dagger\hat{a}\rangle, \langle\hat{b}^\dagger\hat{b}\rangle, \langle\hat{a}^\dagger\hat{b}\rangle, \langle\hat{a}\,\hat{b}\rangle, \langle\hat{a}^2\rangle, \langle\hat{b}^2\rangle$. Starting from the master equation, we obtain a set of differential equations for the mean values of the second-order moments as

$$\begin{aligned}
\frac{d}{dt}\langle\hat{a}^\dagger\hat{a}\rangle &= -ig\langle(\hat{a}^\dagger - \hat{a})(\hat{b}^\dagger + \hat{b})\rangle - \kappa\langle\hat{a}^\dagger\hat{a}\rangle,\\
\frac{d}{dt}\langle\hat{b}^\dagger\hat{b}\rangle &= \quad -ig\langle(\hat{a}^\dagger + \hat{a})(\hat{b}^\dagger - \hat{b})\rangle - \gamma_m\langle\hat{b}^\dagger\hat{b}\rangle + \gamma_m n_m,\\
\frac{d}{dt}\langle\hat{a}^\dagger\hat{b}\rangle &= -\frac{\gamma_m+\kappa}{2}\langle\hat{a}^\dagger\hat{b}\rangle - ig[\langle(\hat{a}^\dagger)^2\rangle - \langle(\hat{b}^\dagger)^2\rangle\\
&\quad - \langle\hat{b}^\dagger\hat{b}\rangle + \langle\hat{a}^\dagger\hat{a}\rangle],\\
\frac{d}{dt}\langle\hat{a}\,\hat{b}\rangle &= \left[-i(\omega_m+\Delta) - \frac{\gamma_m+\kappa}{2}\right]\langle\hat{a}\,\hat{b}\rangle - ig[1 + \langle\hat{b}^2\rangle\\
&\quad + \langle\hat{a}^2\rangle + \langle\hat{a}^\dagger\hat{a}\rangle + \langle\hat{b}^\dagger\hat{b}\rangle],\\
\frac{d}{dt}\langle\hat{a}^2\rangle &= -2ig\langle(\hat{b}^\dagger + \hat{b})\hat{a}\rangle - [\kappa + 2i\Delta]\langle\hat{a}^2\rangle,\\
\frac{d}{dt}\langle\hat{b}^2\rangle &= -2ig\langle(\hat{a}^\dagger + \hat{a})\hat{b}\rangle - [\gamma_m + 2i\omega_m]\langle\hat{b}^2\rangle.
\end{aligned} \tag{7}$$

The steady-state solution of these equations then yields an analytical formula for the final occupancy of the mechanical mode. In the weak coupling regime, i.e., $g \ll \kappa$, the final phonon number is

$$n_f \simeq \frac{\gamma_m n_{\rm th}}{\Gamma + \gamma_m} + \frac{\kappa^2}{16\omega_m^2}, \qquad \Gamma = 4g^2/\kappa, \tag{8}$$

while in the strong coupling regime, i.e., $\kappa \ll g \ll \omega_m$, the final phonon number is

$$n_f \simeq \frac{\gamma_m n_{\rm th}}{\kappa + \gamma_m} + \frac{g^2}{2[\omega_m^2 - 4g^2]}. \tag{9}$$

In this work, we focus on the strong coupling regime. With the given experimental parameters in the main text, we obtain the final phonon number $n_f \sim 0.3$ for the vibration mode, which is well in the quantum ground state. This result is also verified based on numerically solving the quantum master equation (6) (Fig. 3), from which we find that the mechanical mode will enter the quantum ground state at the time $t \sim 100\ \mu$s [Fig. 3(a)].

In the experiment, the diamond beam will need to be sufficiently isolated from other mechanical modes that it can be cooled to its ground state. We now consider the influence of other mechanical modes on the cooling process of the fundamental mode. From the Euler-Bernoulli theory, we know that the first two vibrating modes have the resonance frequencies [54]

$$\omega_m = \frac{4.73^2}{l^2}\sqrt{\frac{EI}{\rho A}},$$
$$\omega_1 = \frac{7.85^2}{l^2}\sqrt{\frac{EI}{\rho A}}. \tag{10}$$

Therefore, if the detuning between these modes is sufficiently large, i.e., $\delta = \omega_1 - \omega_m \gg g$, then we can safely ignore the coupling between the cavity mode and other mechanical modes. One can find that $\omega_1 \sim 3\omega_m$, and $\delta \sim 2\omega_m \sim 4$ MHz, which is much larger than the vibration-photon coupling strength. Thus, we need only to consider the coupling between the fundamental mechanical mode and the cavity photons. Provided that $\omega_1 - \omega_m \gg g$, the diamond resonator will be sufficiently isolated from other mechanical modes. Cooling of the mechanical resonators to the quantum ground state has been realized in a

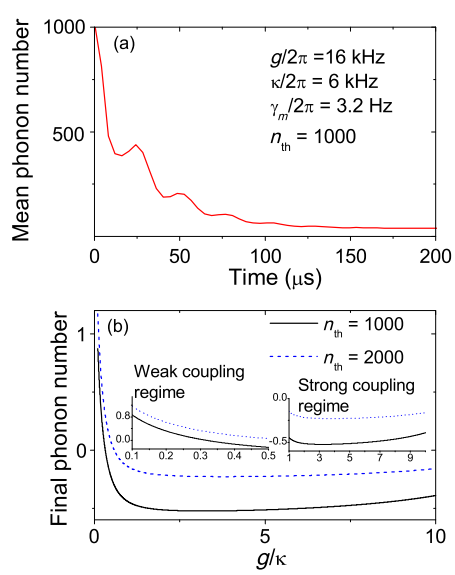

FIG. 3. (a) Time evolution of the mean phonon number from numerically solving the master equation (6) under realistic parameters. (b) The final phonon number in a logarithmic scale as a function of g/κ. The parameters are chosen as those in (a).

variety of experiments exploiting the cavity-assisted sideband cooling approach [61,62]. We believe that cooling the diamond resonators via the same approach, as described in this work, could be realized in the near future with the state-of-the-art technology.

D. Spin-motion couplings

We now turn to considering the coupling between the *NV* center spin and the mechanical motion. Quantum interface between the spin and the CPW cavity can be achieved through a Jaynes-Cummings (JC) spin-motion interaction under a large magnetic-field gradient [51,63–65].

NV centers have a $S = 1$ ground state, with zero-field splitting $D = 2\pi \times 2.87$ GHz between the $|m_s = \pm 1\rangle$ and $|m_s = 0\rangle$ states. We consider a single *NV* center embedded in the thin diamond beam, with its *NV* axis along the z axis. An external magnetic field composed of a homogeneous bias field and a local linear gradient is applied to the system, i.e., $\vec{B}_{NV} = B_0\vec{e}_z + (\partial B/\partial x)x\vec{e}_x$. The homogeneous bias field is used to lift the degeneracy of states $|m_s = +1\rangle$ and $|m_s = -1\rangle$, while the local magnetic-field gradient is used to couple the mechanical motion of the beam to the $S = 1$ spin of the *NV* center. The magnetic-field gradient can be achieved by a single-domain ferromagnet such as Co nanobars near the *NV* center [51,63–65]. In a realistic setup, an objective lens and a laser are needed for optically pumping the spin state of the *NV* center.

The Hamiltonian for the spin-motion coupling system then is $\hat{H}_{NV} = \hbar D S_z^2 + \hbar\omega_m \hat{b}^\dagger \hat{b} + g_{NV}\mu_B \vec{S}\cdot\vec{B}_{NV}$, with $g_{NV} = 2$ the Landé factor of the *NV* center, μ_B the Bohr magneton, and $\vec{S}$ the spin operator for the *NV* center. When $D - g_{NV}\mu_B B_0/\hbar - \omega_m = \delta \ll g_{NV}\mu_B B_0/\hbar$, we can make the rotating-wave approximation to describe the near-resonance interaction between the *NV* spin and the vibration mode and neglect the far-out-of-resonance state $|m_s = +1\rangle$. In this case, the JC Hamiltonian describing the spin-motion dynamics reads [54]

$$\mathcal{H}_2 = \frac{1}{2}\hbar\omega_+\hat{\sigma}_z + \hbar\omega_m \hat{b}^\dagger\hat{b} + \hbar\lambda\hat{b}\hat{\sigma}_+ + \hbar\lambda\hat{b}^\dagger\hat{\sigma}_-, \quad (11)$$

where $\omega_+ = D - g_{NV}\mu_B B_0/\hbar$, $\hat{\sigma}_z = |-1\rangle\langle -1| - |0\rangle\langle 0|$, $\hat{\sigma}_+ = |-1\rangle\langle 0|$, $\hat{\sigma}_- = |0\rangle\langle -1|$, and $\lambda = (g_{NV}\mu_B/\sqrt{2}\hbar)\times(\partial B/\partial x)\sqrt{\hbar/2m\omega_m}$. Using dressed state qubits [51] would be an equivalent alternative approach for implementing this model, which however would need microwave driving of the *NV* spin states.

III. REALISTIC CONSIDERATIONS AND EXPERIMENTAL PARAMETERS

Putting everything together, the total Hamiltonian describing the spin-mechanics-cavity hybrid tripartite system is

$$\mathcal{H} = \frac{1}{2}\hbar\omega_+\hat{\sigma}_z + \hbar\omega_m\hat{b}^\dagger\hat{b} + \hbar\Delta\hat{a}^\dagger\hat{a} + \hbar g\hat{a}^\dagger\hat{b} + \hbar g\hat{a}\hat{b}^\dagger + \hbar\lambda\hat{b}\hat{\sigma}_+ + \hbar\lambda\hat{b}^\dagger\hat{\sigma}_-. \quad (12)$$

The first three terms describe the free Hamiltonian for the spin, the phonons, and the photons, while the last four terms describe the coherent coupling of the phonons to both the spin and the photons. In a realistic experimental situation, we need to consider cavity photon loss, mechanical dissipation, and spin dephasing. The full dynamics of our system that takes these incoherent processes into account is described by the master equation

$$\frac{d\hat{\rho}(t)}{dt} = -\frac{i}{\hbar}[\mathcal{H},\hat{\rho}] + \kappa\mathcal{D}[\hat{a}]\hat{\rho} + \gamma_s\mathcal{D}[\hat{\sigma}_z]\hat{\rho} + n_{\rm th}\gamma_m\mathcal{D}[\hat{b}^\dagger] + (n_{\rm th}+1)\gamma_m\mathcal{D}[\hat{b}] \quad (13)$$

with γ_s the single spin dephasing rate of the *NV* center. To enter the strong coupling regime requires that $\{g,\lambda\} > \{n_{\rm th}\gamma_m, \kappa, \gamma_s\}$.

Let us consider the experimental feasibility in the configuration as shown in Fig. 1 and the appropriate parameters to achieve strong coupling. (i) For a CPW cavity with strip-line length $L \sim 1$ cm, electrode distance $d \sim 5\ \mu$m, and effective dielectric constant $\epsilon_{\rm eff} \sim 6$, the mode frequency for the CPW cavity is $\omega_c = \pi c/L\sqrt{\epsilon_{\rm eff}} \sim 2\pi \times 6$ GHz. With the above parameters for the CPW cavity, the electric-field amplitude of a single photon is $\mathcal{E}_0 \sim 0.76$ V/m. If the beam is positioned at a distance of about 1 μm above the CPW surface gap, then we can estimate the mode function as $|\vec{e}_{\rm tr}(x_0,y_0)| \sim e^{-0.2}$ and $[\partial_x\vec{e}_{\rm tr}(x,y)]_{(x_0,y_0)} \sim (2\ \mu{\rm m})^{-1}$, respectively [see Fig. 2(c)]. (ii) We consider a diamond microbeam of cross-sectional radius $r \sim 100$ nm under a strong ac electric field with $E_p \sim 10$ V/μm and a gradient magnetic field with $\partial_x B \sim 10^7$ T/m [54]. Figure 4 shows the calculated coupling strengths as a function of the length of the diamond beam with the given parameters. We find that the optimal length of the beam under the given parameters is about

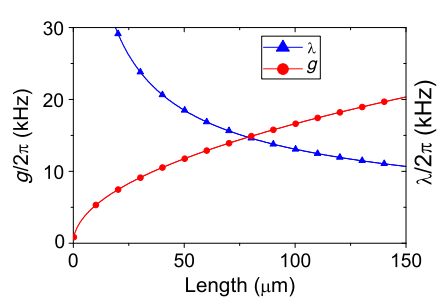

FIG. 4. Photon-motion coupling strength g and spin-motion coupling strength λ as a function of the length of the diamond beam. The relevant parameters are $r \sim 100$ nm, $\mathcal{E}_0 \sim 0.76$ V/m, $[\partial_x\vec{e}_{\rm tr}(x,y)]_{(x_0,y_0)} \sim (2\,\mu{\rm m})^{-1}$, $E_p \sim 10$ V/μm, and $\partial_x B \sim 10^7$ T/m.

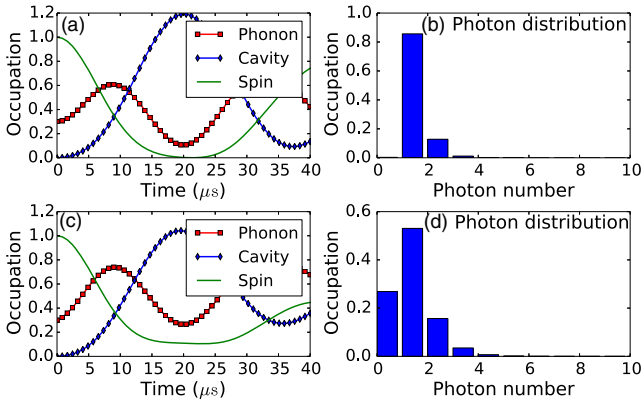

FIG. 5. (a) Vacuum Rabi oscillations of the hybrid system where the mechanical resonator couples to the spin and the cavity without dissipations. The initial state of the beam is a thermal state with $n_m \sim 0.3$, while the spin is initially in the spin-up state and the cavity in the ground state. (b) Photon distribution in the cavity after a half period of Rabi oscillations. (c),(d) The same as (a),(b) but with dissipations for the spin, the mechanical resonator, and the cavity. The relevant parameters are $g/2\pi \sim 16$ kHz, $\lambda/2\pi \sim 16$ kHz, $\kappa/2\pi \sim 6$ kHz, $n_{\rm th} \sim 1000$, $\gamma_m/2\pi \sim 3.2$ Hz, and $\gamma_s/2\pi \sim 2$ kHz.

$l \sim 80$ μm. The vibration frequency for the fundamental mode is $\omega_m/2\pi \sim 320$ kHz. Then, the photon-motion and spin-motion coupling strengths can reach $g/2\pi \sim 16$ kHz and $\lambda/2\pi \sim 16$ kHz, respectively.

We next turn to damping of the mechanical motion. For a diamond beam with frequency ω_m and quality factor Q, the mechanical damping rate is $\gamma_m = \omega_m/Q$. The recent demonstration of high-quality single-crystal diamond beams or cantilevers with embedded NV centers leads to a mechanical quality factor exceeding 10^5 [38–44]. For our doubly clamped diamond beam with vibration frequency $\omega_m/2\pi \sim 320$ kHz, the damping rate is about $\gamma_m/2\pi \sim 3.2$ Hz and to ensure the strong coupling condition thus requires that $n_{\rm th} < 5000$. For the mechanical mode of frequency $\omega_m/2\pi \sim 320$ kHz, assuming an environmental temperature $T \sim 20$ mK in a dilution refrigerator, the thermal phonon number is about $n_{\rm th} \sim 10^3$. To keep the mechanical motion in the quantum ground state thus needs additional cooling.

Finally, we consider the cavity photon loss and the dephasing of the NV spin. For a realistic value of the quality factor for the CPW cavity $Q \sim 10^6$, the photon decay rate is about $\kappa/2\pi \sim 6$ kHz. In the experiment, superconducting cavities are able to maintain high Q even at applied in-plane magnetic fields > 200 mT [18–20]. Therefore, we can safely ignore the effect of ultrastrong nanomagnets in close proximity to superconducting CPW cavities. When it comes to the NV center, the dephasing time T_2 induced by the fluctuations in the nuclear spin bath can be increased to several milliseconds in ultrapure diamond [66]. We can ignore single spin relaxation as T_1 can be several minutes at low temperatures. The effect of other centers coupled to the mechanical motion of the beam can be neglected [54].

Figure 5 shows the numerical simulations of quantum dynamics of the spin-mechanics-cavity system through solving the master equation (6). We find that, with the given parameters, the coherent interactions can dominate the decoherence processes in the hybrid setup, which enables the strong coupling regime to be entered. In this regime, the mechanical motion becomes strongly coupled to the spin and the cavity photons in direct analogy to strong coupling of cavity QED.

IV. APPLICATIONS

A. Quantum state transfer via dark polaritons

In general, the spin-electromechanical hybrid tripartite system modeled by the Hamiltonian (12) can find use in many aspects of quantum science and technology. In the following, we propose to realize coherent information transfer between the single spin and the microwave cavity, using mechanically dark polaritons. This method is very efficient and robust against mechanical noise compared to the direct-transfer process, since, during the state conversion process, the mechanical mode is decoupled from the dark polaritons composed of the spin and the cavity modes.

We proceed by assuming that $\omega_+ \sim \Delta \sim \omega_m = \Omega$. Then, it can readily be verified that the Hamiltonian (12) can take a compact form in terms of spin-photon polariton and spin-photon-phonon polaron operators

$$\mathcal{H} = \hbar\Omega\mathcal{P}_d^\dagger\mathcal{P}_d + \hbar\Omega_+\mathcal{P}_+^\dagger\mathcal{P}_+ + \hbar\Omega_-\mathcal{P}_-^\dagger\mathcal{P}_-, \quad (14)$$

with $\mathcal{P}_d = \cos\theta\hat{\sigma}_- - \sin\theta\hat{a}, \tan\theta = \lambda/g$ being the polariton operator, describing quasiparticles formed by combinations of spin and photon excitations, and $\mathcal{P}_\pm = (1/\sqrt{2})(\mathcal{P}_b \pm \hat{b})$, $\mathcal{P}_b = \cos\theta\hat{a} + \sin\theta\hat{\sigma}_-$, describing polarons formed by combinations of polariton and phonon excitations. The frequencies of the polarons are $\Omega_\pm = \Omega \pm \sqrt{g^2+\lambda^2}$. We refer to $\mathcal{P}_d$ as the *mechanically dark polariton* operator, due to the fact that it is decoupled from the mechanical mode, independently of the couplings. The mechanically dark polaritons can find use in quantum state conversion between the spin and cavity photons. This task can be accomplished through using an adiabatic passage approach, similar to the well-known STIRAP scheme [67–70]. By simply making $g(t)$ initially bigger than λ, but keeping λ finite, one can modulate the coupling strengths $g(t)$ slowly to ensure that the system adiabatically follows the dark polaritons. This will adiabatically rotate the mixing angle θ from 0 to $\pi/2$, leading to a complete and reversible transfer of the spin state to the photonic state; i.e., the dark polariton operator adiabatically evolves from being $\hat{\sigma}_-$ at $t = 0$ to $-\hat{a}$ at the end of the protocol at a time $t = t_f$.

In Fig. 6, we display the numerical results for the state conversion process using dark polaritons through solving the master equation (6). The initial spin state is chosen as $(1/\sqrt{2})(|0\rangle + |-1\rangle)$, while the cavity state is initially in the ground state and the mechanical mode is initially in the thermal state with $n_m = 0.1$. At the end of the transfer process, the cavity state is steered into $(1/\sqrt{2})(|0\rangle + |1\rangle)$ with a fidelity above 90%. This fidelity could further be improved with optimized pulses for $g(t)$ and detunings. In the simulations, we choose the time dependence for the coupling g as exponential, but this pulse form is not necessarily required. The polarization coupling strength g is proportional to the classical electric field $\vec{E}_p(t)$, which can be tailored to give the desired time-dependent form. The spin state thus can be transferred from the *NV* center to the photonic state in the CPW cavity using the mechanical motion but without actually populating it. Therefore, this approach offers a distinct feature that the state transfer process exploiting dark polaritons is highly immune to mechanical noises.

B. Effective strong coupling between the spin and the CPW cavity

Alternatively, one can detune the mechanical mode and couple the spin to the microwave field via virtual motional excitations. In general, the direct coupling between a single *NV* spin and the microwave-cavity field is inherently rather weak. Here we propose to reach the effective strong coupling regime with this hybrid spin-electromechanical system. The induced effective strong coupling offers great potential for single-photon manipulation in the microwave frequency domain with this hybrid architecture.

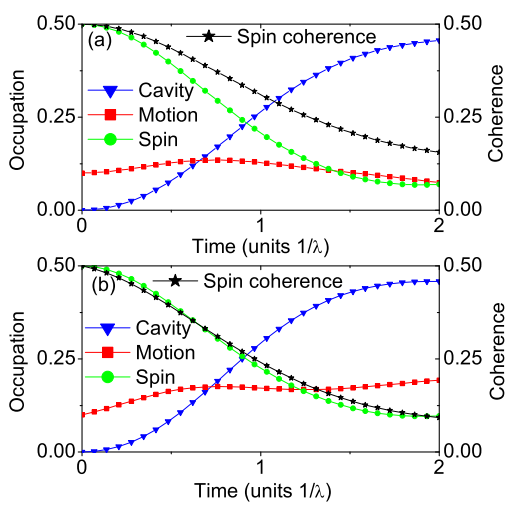

FIG. 6. (a) Adiabatic population transfer without dissipations. (b) The same as (a) but with dissipations for the spin, the mechanical resonator, and the cavity. Relevant parameters are $g = g_0 e^{-t^2/4}$, $g_0 = 1.8\lambda$, $\kappa = 0.1\lambda, \gamma_m = 0.0001\lambda$, $n_{\rm th} = 1000$, and $\gamma_s = 0.1\lambda$.

In the frame rotating at the spin's resonance frequency ω_+, the Hamiltonian of the hybrid system is given by

$$\mathcal{H} = \hbar\Delta_1 \hat{b}^\dagger \hat{b} + \hbar\Delta_2 \hat{a}^\dagger \hat{a} + \hbar g \hat{a}^\dagger \hat{b} + \hbar g \hat{a} \hat{b}^\dagger + \hbar\lambda \hat{b}\hat{\sigma}_+ + \hbar\lambda \hat{b}^\dagger \hat{\sigma}_-, \tag{15}$$

where $\Delta_1 = \omega_m - \omega_+$ and $\Delta_2 = \Delta - \omega_+$. Taking the dissipations into consideration, the system is described by the quantum master equation

$$\frac{d\hat{\rho}(t)}{dt} = -\frac{i}{\hbar}[\mathcal{H}, \hat{\rho}] + \kappa\mathcal{D}[\hat{a}]\hat{\rho} + \gamma_s \mathcal{D}[\hat{\sigma}_z]\hat{\rho} + n_{\rm th}\gamma_m \mathcal{D}[\hat{b}^\dagger] + (n_{\rm th} + 1)\gamma_m \mathcal{D}[\hat{b}]. \tag{16}$$

By adiabatically eliminating the mechanical mode $\hat{b}$ for large detunings, $\Delta_1, \Delta_2 \gg g, \lambda$, virtual excitations of the mechanical mode result in an effective interaction between the *NV* spin and the CPW cavity mode $\hat{a}$, with the effective Hamiltonian

$$\mathcal{H}_{\rm eff} = \hbar(\Delta_2 - \beta^2\Delta_1)\hat{a}^\dagger \hat{a} - \frac{1}{2}\alpha^2 \Delta_1 \hat{\sigma}_z + \hbar g_{\rm eff} \hat{a}^\dagger \hat{\sigma}_- + \hbar g_{\rm eff} \hat{a}\hat{\sigma}_+, \tag{17}$$

where the parameters $\alpha = \lambda/\Delta_1$, $\beta = g/\Delta_1$, and the effective spin-photon coupling strength $g_{\rm eff} = \alpha g$. Then the reduced density matrix for the spin-cavity system will satisfy the effective master equation

$$\frac{d\hat{\varrho}(t)}{dt} = -\frac{i}{\hbar}[\mathcal{H}_{\rm eff}, \hat{\varrho}] + \kappa^1_{\rm eff}\mathcal{D}[\hat{a}]\hat{\varrho} + \gamma_s \mathcal{D}[\hat{\sigma}_z]\hat{\rho} + \gamma^1_{\rm eff}\mathcal{D}[\hat{\sigma}_-]\hat{\varrho} + \kappa^2_{\rm eff}\mathcal{D}[\hat{a}^\dagger]\hat{\varrho} + \gamma^2_{\rm eff}\mathcal{D}[\hat{\sigma}_+]\hat{\varrho}. \tag{18}$$

The effective decay rates of the cavity mode and the *NV* spin are described by $\kappa^1_{\rm eff} = \kappa + \beta^2(n_{\rm th} + 1)\gamma_m$, $\kappa^2_{\rm eff} = \beta^2 n_{\rm th}\gamma_m$ and $\gamma^1_{\rm eff} = \alpha^2(n_{\rm th} + 1)\gamma_m$, $\gamma^2_{\rm eff} = \alpha^2 n_{\rm th}\gamma_m$, respectively. It can be easily found that the effective coupling strength $g_{\rm eff}$ depends linearly on α, while the effective decay rates $\kappa^i_{\rm eff}$ and $\gamma^i_{\rm eff}$ are quadratic functions of the parameters α and β. Therefore, the spin-cavity coupled system can be steered into the strong coupling regime if $\{\alpha, \beta\} \ll 1$ and $\{\kappa, \gamma_s\} < g_{\rm eff}$; i.e., the effective coupling strength can exceed the decay rates $g_{\rm eff} > \gamma_s, \kappa^i_{\rm eff}, \gamma^i_{\rm eff}$, $i = 1, 2$.

We now consider the relevant parameters to reach the effective strong coupling. Taking $\Delta_1 \simeq \Delta_2 = \Delta, g \simeq \lambda$, $\Delta = 10g$, one can get $g_{\rm eff} = 0.1g$, $\kappa^1_{\rm eff} \simeq \kappa$, $\kappa^2_{\rm eff} \simeq 0$, $\gamma^1_{\rm eff} \simeq \gamma^2_{\rm eff} \simeq 0$. Then the effective master equation describing the spin-cavity system reads

$$\frac{d\hat{\varrho}(t)}{dt} = -\frac{i}{\hbar}[\mathcal{H}_{\rm eff}, \hat{\varrho}] + \kappa\mathcal{D}[\hat{a}]\hat{\varrho} + \gamma_s \mathcal{D}[\hat{\sigma}_z]\hat{\rho}. \tag{19}$$

So the effective strong coupling regime requires $g_{\rm eff} > \kappa, \gamma_s$, which means $g, \lambda \geq 10\kappa, 10\gamma_s$.

We now estimate the coupling strengths in the configuration shown in Figs. 1(c) and 1(d). For the CPW cavity considered in this work, $u_0 \sim 5\ \mu$V. We consider a diamond microbeam of cross-sectional radius $r \sim 50$ nm and length approximately 1 μm. Taking $\zeta \sim 0.4$ and $h \sim 100$ nm, then we have $g/2\pi \sim 60$ kHz and $\lambda/2\pi \sim 40$ kHz. Then if we take $\Delta/2\pi \sim 300$ kHz, we can obtain $g_{\rm eff}/2\pi \sim 10$ kHz. This effective coupling strength can exceed the decay rates of a CPW cavity with a quality factor $Q > 10^6$. Magnetic coupling between a spin ensemble and a superconducting cavity has been reported recently [18–20], but the coupling between a single *NV* spin and the microwave-cavity field is inherently rather weak. Here we have proposed an efficient method to reach the effective strong coupling regime with this hybrid spin-electromechanical system. The resulting effective coupling strength can be significantly enhanced by approximately 3 orders of magnitude.

Related schemes have been investigated before for interfacing a single spin to a transmission line cavity [22,46]. Different fundamentally from these proposals, here we specifically exploit the dielectric interaction through an ac electric field and state transfer schemes via mechanically dark polaritons. Both techniques are, in particular, useful to realize such interactions with *NV* centers in diamond beams, a system which is currently very actively explored in this context [38–44]. Furthermore, our proposed device just requires placing the diamond beam above the CPW surface, with no need to integrate the diamond resonator into the tiny coupling capacitor. This design is thus much easier to implement in practice and possesses the advantage of scalability, particularly for much bigger diamond microbeams.

V. CONCLUSIONS

We present a spin-mechanics-cavity hybrid device where a vibrating diamond beam with implanted single *NV* spins is coupled to a superconducting CPW cavity. We show that, under an ac electric field, the diamond beam can strongly couple to the CPW cavity through dielectric interaction. Together with the strong spin-motion interaction via a large magnetic-field gradient, it provides a hybrid quantum device where the diamond resonator can strongly couple both to the single microwave-cavity photons and to the single *NV* center spin. The distinct feature of this device is that it is on chip and scalable to large arrays of mechanical resonators coupled to the same CPW cavity. As for applications, we propose to use this hybrid setup to implement quantum-information transfer between the *NV* spin and the CPW cavity via mechanically dark polaritons. This hybrid spin-electromechanical device can offer a realistic platform for implementing quantum information with single *NV* spins, mechanical resonators, and single microwave photons.

ACKNOWLEDGMENTS

This work is supported by the NSFC under Grants No. 11474227 and No. 11534008 and the Fundamental Research Funds for the Central Universities. Part of the simulations are coded in PYTHON using the QUTIP library [71]. Work at Vienna is supported by the WWTF, the Austrian Science Fund (FWF) through SFB FOQUS, and the START Grant No. Y 591-N16 and the European Commission through Marie Sklodowska-Curie Grant No. IF 657788.

APPENDIX A: DIELECTRIC COUPLINGS

1. Fundamental vibration mode of the diamond beam

For a thin beam, the Euler-Bernoulli elastic theory is valid [72,73]. We consider a doubly clamped diamond beam with dimensions $l \gg r$. The equation for the lateral vibration of a thin beam is

$$\rho A \frac{\partial^2}{\partial t^2}\phi(z,t) + EI\frac{\partial^4}{\partial z^4}\phi(z,t) = 0, \tag{A1}$$

where $\phi(z,t)$ is the lateral displacement in the x direction, A is the beam cross section, and I is the moment of inertia, $I = \pi r^4/8$ for a cylindrical beam. The solutions to this equation are $\phi(z,t) = u(z)e^{-i\omega t}$, with the mode function

$$u(z) = C_1(\cos kz - \cosh kz) + C_2(\sin kz - \sinh kz), \tag{A2}$$

which satisfies the boundary conditions $u(0) = u(l) = 0$, $u'(0) = u'(l) = 0$ for a doubly clamped beam. The frequency equation is given by

$$\cos kl \cosh kl = 0. \tag{A3}$$

The first five nontrivial consecutive roots of this equation are given below:

$k_0 l$	$k_1 l$	$k_2 l$	$k_3 l$	$k_4 l$
4.730	7.853	10.996	14.137	17.279

and the corresponding eigenfrequencies are

$$\omega_n = k_n^2\sqrt{\frac{EI}{\rho A}}. \tag{A4}$$

Therefore, the fundamental mode has the vibration frequency $\omega_m = (4.73^2/l^2)\sqrt{EI/\rho A}$.

2. CPW cavity-field operator

For a CPW cavity as shown in Fig. 1 of the main text, the coplanar waveguide problem can be reduced to a rectangular waveguide problem by inserting magnetic walls at

$y = 0$ and $y = b$ and electric walls at $z = 0$ and $z = L$ [74,75]. If the central conductor is interrupted by two capacitors or gaps with a strip-line distance L, the cavity modes will be standing waves in the axial direction. Then, the classical electric-field components are given by [74,75]

$$E_x = -\sum_n \left\{ \mathcal{E}_0 \frac{1}{F_n} \left[\frac{\sin\frac{n\pi\delta}{2}}{\frac{n\pi}{2}\delta} \sin\frac{n\pi\bar{\delta}}{2} \right] \cos\frac{n\pi y}{b} e^{-\gamma_n x} \right\} \times \cos\frac{m\pi z}{L}, \tag{A5}$$

$$E_y = \sum_n \left\{ \mathcal{E}_0 \left[\frac{\sin\frac{n\pi\delta}{2}}{\frac{n\pi}{2}\delta} \sin\frac{n\pi\bar{\delta}}{2} \right] \sin\frac{n\pi y}{b} e^{-\gamma_n x} \right\} \times \cos\frac{m\pi z}{L}, \tag{A6}$$

$$E_z = 0, \tag{A7}$$

where $\delta = d/b$, $\bar{\delta} \sim \delta$, $F_n = (b\gamma_n/n\pi) = \sqrt{1 + (2bv/n\lambda_0)^2}$, $v = \sqrt{(\lambda_0/\lambda_c)^2 - 1}$, and λ_0 is the free space wavelength for the mode frequency ω_c. The cavity wavelength λ_c is related to the free space wavelength λ_0 with the expression $\lambda_c = \lambda_0/\sqrt{\epsilon_{\text{eff}}}$, where ϵ_{eff} is the effective relative dielectric constant.

The diamond beam positioned a few micrometers above the gap will experience the very strong localized electric field of the CPW cavity. In this work, we take the half-wavelength mode with $m = 1$, in which case the cavity wavelength is $\lambda_c = 2L$. Following the standard procedure for quantizing the electromagnetic fields, we obtain the quantized form of the single-mode electric-field operator for the CPW cavity:

$$\hat{\vec{E}}(\vec{r}, t) = \mathcal{E}_0 \vec{e}_{\text{tr}}(x, y)(\hat{a} e^{-i\omega_c t} + \hat{a}^\dagger e^{i\omega_c t}) \cos\frac{\pi z}{L}, \tag{A8}$$

where the transverse mode function is

$$\vec{e}_{\text{tr}}(x, y) = -\sum_n \left\{ \frac{1}{F_n} \left[\frac{\sin\frac{n\pi\delta}{2}}{\frac{n\pi}{2}\delta} \sin\frac{n\pi\bar{\delta}}{2} \right] \cos\frac{n\pi y}{b} e^{-\gamma_n x} \right\} \vec{e}_x + \sum_n \left\{ \left[\frac{\sin\frac{n\pi\delta}{2}}{\frac{n\pi}{2}\delta} \sin\frac{n\pi\bar{\delta}}{2} \right] \sin\frac{n\pi y}{b} e^{-\gamma_n x} \right\} \vec{e}_y \tag{A9}$$

and $\vec{e}_x$ and $\vec{e}_y$ are the unit vectors for the x and y axes, respectively. Then the electric-field operator in the position of the diamond beam is

$$\hat{\vec{E}}(\vec{r}_{\text{dm}}, t) = \mathcal{E}_0 \vec{e}_{\text{tr}}(x_0, y_0)(\hat{a} e^{-i\omega_c t} + \hat{a}^\dagger e^{i\omega_c t}), \tag{A10}$$

where we assume that the beam is positioned at the maximum slope of the standing wave mode, i.e., $\cos(\pi z_0/L) = 1$. For the case that the beam is positioned at a distance of several micrometers above the cavity gap, from numerical simulations we find that the mode function can be approximated as $|\vec{e}_{\text{tr}}(x_0, y_0)| \sim e^{-1}$, and $[\partial_x \vec{e}_{\text{tr}}(x, y)]_{(x_0, y_0)} \sim \gamma \sim (5\ \mu\text{m})^{-1}$.

3. Cavity-resonator couplings

For a thin beam with a circular cross section, it lacks a closed-form expression for the polarizability tenser. However, it has been shown that the analytical expression for the polarizability of a spheroid can be very close to that of a cylinder of the same permittivity ϵ and aspect ratio [55]. In the following, we employ the polarizability tenser of a thin prolate spheroid instead. Considering the case where the dimension of the diamond beam is much smaller than the wavelength of the electric field, its dielectric response is well approximated by a point dipole:

$$\vec{p}(\vec{r}') = V\alpha_\perp \vec{E}_\perp(\vec{r})\delta(\vec{r} - \vec{r}'). \tag{A11}$$

In this case, the Hamiltonian describing the electrostatic interaction between the microbeam and the electric field is

$$\hat{H}_{\text{pol}} = -\frac{1}{2} V\alpha_\perp |\vec{E}_\perp(\vec{r}_{\text{dm}}, t)|^2. \tag{A12}$$

As the beam vibrates, the cavity electric field affected by the beam will be modulated by the vibration. Expanding the cavity-field operator around the position of the beam up to first order in the transverse displacement operator $\hat{q}_x$ and neglecting rapidly oscillating and other higher-order terms, the Hamiltonian describing the coupled system reads

$$\hat{H}_{\text{pol}} = -V\alpha_\perp \vec{E}_p \cdot \vec{E}_c(\vec{r}_0, t) - V\alpha_\perp \vec{E}_p \cdot \partial_x \vec{E}_c(\vec{r}, t)\hat{q}_x. \tag{A13}$$

The first term corresponds to the driving of the cavity mode by the electric dipole, while the second term describes the optomechanical coupling between the vibration and the cavity mode. In order to eliminate the first term, we can simply drive the cavity with a second field with an appropriately chosen amplitude and which is π out of phase with respect to $\vec{E}_p$. Then, the coupling between this dipole and the cavity can cancel the first term in Eq. (A13) as a result of destructive interference between these two coupling terms. In this case, the pure electromechanical coupling of the vibration to the cavity mode can be derived as

$$\begin{aligned} \hat{H}_{\text{pol}} &= -V\alpha_\perp \mathcal{E}_0 \vec{E}_p \cdot [\partial_x \vec{e}_{\text{tr}}(x, y)]_{(x_0, y_0)} (e^{i\omega_p t} + e^{-i\omega_p t}) \\ &\quad \times (\hat{a} e^{-i\omega_c t} + \hat{a}^\dagger e^{i\omega_c t})\hat{q}_x \\ &= -V\alpha_\perp \mathcal{E}_0 \vec{E}_p \cdot [\partial_x \vec{e}_{\text{tr}}(x, y)]_{(x_0, y_0)} (\hat{a} e^{i\Delta t} + \hat{a}^\dagger e^{-i\Delta t})\hat{q}_x. \end{aligned} \tag{A14}$$

After quantizing the vibration mode of the diamond beam, i.e., $\hat{q}_x = \sqrt{\hbar/2m\omega_m}(\hat{b}^\dagger + \hat{b})$, we have

$$\begin{aligned}\hat{H}_{\rm pol} &= -V\alpha_\perp \mathcal{E}_0 \vec{E}_p \cdot [\partial_x \vec{e}_{\rm tr}(x,y)]_{(x_0,y_0)} \sqrt{\frac{\hbar}{2m\omega_m}} \\ &\quad \times (\hat{a}e^{i\Delta t} + \hat{a}^\dagger e^{-i\Delta t})(\hat{b}e^{-i\omega_m t} + \hat{b}^\dagger e^{i\omega_m t}) \\ &= \hbar g(\hat{a}e^{i\Delta t} + \hat{a}^\dagger e^{-i\Delta t})(\hat{b}e^{-i\omega_m t} + \hat{b}^\dagger e^{i\omega_m t}). \end{aligned} \tag{A15}$$

APPENDIX B: SPIN-MOTION COUPLINGS

1. Detailed derivation of the spin-motion interaction Hamiltonian

We consider a single NV center embedded in the microscale diamond beam, with its NV axis along the z direction. NV centers have a $S = 1$ ground state, with zero-field splitting $D = 2\pi \times 2.87$ GHz between the $|m_s = \pm 1\rangle$ and $|m_s = 0\rangle$ states. The Hamiltonian describing the NV center in an external magnetic field $\vec{B}_{NV}$ has the form

$$\hat{H}_{NV} = \hbar D S_z^2 + g_{NV}\mu_B \vec{S} \cdot \vec{B}_{NV}. \tag{B1}$$

We assume that the external magnetic field is composed of a homogeneous bias field and a linear gradient, i.e., $\vec{B}_{NV} = B_0 \vec{e}_z + \partial_x B x \vec{e}_x$. Then, the Hamiltonian (B1) becomes

$$\begin{aligned}\hat{H}_{NV} &= \hbar D S_z^2 + g_{NV}\mu_B B_0 S_z + \Lambda S_x(\hat{b} + \hat{b}^\dagger) \\ &\quad + \hbar\omega_m \hat{b}^\dagger \hat{b}, \end{aligned} \tag{B2}$$

with the spin-motion coupling strength $\Lambda = g_{NV}\mu_B(\partial B/\partial x)\sqrt{\hbar/2m\omega_m}$. In the basis defined by the eigenstates of S_z, i.e., $\{|m_s\rangle, m_s = 0, \pm 1\}$, with $S_z|m_s\rangle = m_s|m_s\rangle$, we have

$$\begin{aligned}\hat{H}_{NV} &= (\hbar D + g_{NV}\mu_B B_0)|+1\rangle\langle +1| \\ &\quad + (\hbar D - g_{NV}\mu_B B_0)|-1\rangle\langle -1| + \hbar\omega_m \hat{b}^\dagger \hat{b} \\ &\quad + \Lambda(\hat{b} + \hat{b}^\dagger)[\langle +1|S_x|0\rangle|+1\rangle\langle 0| \\ &\quad + \langle -1|S_x|0\rangle|-1\rangle\langle 0| + \text{H.c.}]. \end{aligned} \tag{B3}$$

When $D - g_{NV}\mu_B B_0/\hbar - \omega_m = \delta \ll g_{NV}\mu_B B_0/\hbar$, we can make the rotating-wave approximation to describe the near-resonance interaction between the NV spin and the mechanical motion and neglect the far-out-of-resonance state $|m_s = +1\rangle$. Then we can obtain the Hamiltonian describing the spin-motion dynamics

$$\mathcal{H}_2 = \frac{1}{2}\hbar\omega_+ \hat{\sigma}_z + \hbar\omega_m \hat{b}^\dagger \hat{b} + \hbar\lambda \hat{b}\hat{\sigma}_+ + \hbar\lambda \hat{b}^\dagger \hat{\sigma}_-, \tag{B4}$$

where $\omega_+ = D - g_{NV}\mu_B B_0/\hbar$, $\hat{\sigma}_z = |-1\rangle\langle -1| - |0\rangle\langle 0|$, $\hat{\sigma}_+ = |-1\rangle\langle 0|$, $\hat{\sigma}_- = |0\rangle\langle -1|$, and $\lambda = (g_{NV}\mu_B/\sqrt{2}\hbar)\times(\partial B/\partial x)\sqrt{\hbar/2m\omega_m}$.

2. Large magnetic-field gradient induced by a micromagnet

In the main text, the spin-motion coupling between the NV center and the vibration mode needs a large magnetic-field gradient along the x direction. This can be generated by a micromagnet of magnetization $\vec{M}$ oriented along the x axis near the NV center. The micromagnet can be created via lithographic processes, which is a single magnetic domain whose magnetic moment is spontaneously oriented along its long axis due to the shape anisotropy. We consider Co nanobars with dimensions $(l, w, t) = (200, 50, 50)$ nm. Approximating the bar by a magnetic dipole, we have $(\partial B/\partial x) = 3\mu_0|\vec{m}|/4\pi d_0^4$, where $\vec{m} = lwt\vec{M}$ and d_0 is the distance between the tip and the NV spin. Taking $M = 1.5 \times 10^6$ A/m, $d_0 = 60$ nm, we obtain $(\partial B/\partial x) \sim 10^7$ T/m. A large field gradient of such a value is reported in magnetic resonance force microscopy experiments [76].

APPENDIX C: EFFECTS OF OTHER DECOHERENCE PROCESSES

In this Appendix, we consider some other decoherence processes that are less important and have been ignored in the main text. These decoherence processes include scattered photon-recoil heating by dipole radiation and spin relaxation due to strain-induced coupling to the nearby NV centers.

1. Scattered photon-recoil heating by dipole radiation

We now consider the scattered photon-recoil heating of the vibration mode due to dipole radiation. Since the electric dipole moment induced by the strong ac electric field in the diamond beam is oscillating in time, it will radiate photons from the beam in the form of dipole radiation, which in turn causes decoherence to the mechanical motion due to momentum recoil kicks. We assume that each scattered photon contributes the maximum possible momentum kick of $\hbar k$ along the x axis, giving rise to a momentum diffusion process $d\langle p_x^2\rangle/dt = \Gamma_{\rm sc}(\hbar k)^2$, where $\Gamma_{\rm sc}$ is the photon scattering rate. The decay rate $\gamma_{\rm sc}$ associated with scattered photon-recoil heating can be approximated as $\gamma_{\rm sc} \simeq (\omega_r/\omega_m)\Gamma_{\rm sc}$, with $\omega_r = \hbar k^2/(2m)$ the recoil frequency. For dipole radiation, the photon scattering rate $\Gamma_{\rm sc}$ can be calculated by taking the power radiated by the dipole strength $\vec{p}$ and dividing by the energy per photon, i.e., $\Gamma_{\rm sc} = (c^2 Z_0 k^4/12\pi\hbar\omega)|\vec{p}|^2$. For the given parameters, the photon-recoil heating rate is about $\gamma_{\rm sc} \sim 10^{-5}$ Hz, which thus can be neglected.

2. Spin decoherence due to strain-induced coupling between nearby *NV* centers

Let us consider the effect of nearby *NV* centers on this *NV* center spin via strain-induced couplings. When the beam vibrates, it strains the diamond lattice, which in turn couples directly to the spin-triplet states in the *NV* electronic ground state. It has been shown that [25] this strain-induced spin-phonon coupling can lead to effective spin-spin interactions mediated by virtual phonons. This phonon-mediated spin-spin coupling strength is about $2g^2/\Delta$, where g is the coupling strength between a single *NV* spin and a single phonon via strains and Δ is frequency detuning. For the diamond beam considered in this work, the single phonon coupling is very weak, $g \sim 1$ Hz. Thus, the phonon-mediated spin-spin couplings can be completely ignored.

[1] Ze-Liang Xiang, Sahel Ashhab, J. Q. You, and Franco Nori, Hybrid quantum circuits: Superconducting circuits interacting with other quantum systems, Rev. Mod. Phys. **85**, 623 (2013).

[2] J. Verdú, H. Zoubi, Ch. Koller, J. Majer, H. Ritsch, and J. Schmiedmayer, Strong Magnetic Coupling of an Ultracold Gas to a Superconducting Waveguide Cavity, Phys. Rev. Lett. **103**, 043603 (2009).

[3] Peng-Bo Li and Fu-Li Li, Controlled generation of field squeezing with cold atomic clouds coupled to a superconducting transmission line resonator, Phys. Rev. A **81**, 035802 (2010).

[4] Anders S. Sørensen, Caspar H. van der Wal, Lilian I. Childress, and Mikhail D. Lukin, Capacitive Coupling of Atomic Systems to Mesoscopic Conductors, Phys. Rev. Lett. **92**, 063601 (2004).

[5] D. Petrosyan and M. Fleischhauer, Quantum Information Processing with Single Photons and Atomic Ensembles in Microwave Coplanar Waveguide Resonators, Phys. Rev. Lett. **100**, 170501 (2008).

[6] D. Kielpinski, D. Kafri, M. J. Woolley, G. J. Milburn, and J. M. Taylor, Quantum Interface between an Electrical Circuit and a Single Atom, Phys. Rev. Lett. **108**, 130504 (2012).

[7] Z. Darázs, Z. Kurucz, O. Kálmán, T. Kiss, J. Fortágh, and P. Domokos, Parametric Amplification of the Mechanical Vibrations of a Suspended Nanowire by Magnetic Coupling to a Bose-Einstein Condensate, Phys. Rev. Lett. **112**, 133603 (2014).

[8] A. André, D. DeMille, J. M. Doyle, M. D. Lukin, S. E. Maxwell, P. Rabl, R. J. Schoelkopf, and P. Zoller, A coherent all-electrical interface between polar molecules and mesoscopic superconducting resonators, Nat. Phys. **2**, 636 (2006).

[9] P. Rabl, D. DeMille, J. M. Doyle, M. D. Lukin, R. J. Schoelkopf, and P. Zoller, Hybrid Quantum Processors: Molecular Ensembles as Quantum Memory for Solid State Circuits, Phys. Rev. Lett. **97**, 033003 (2006).

[10] Karl Tordrup, Antonio Negretti, and Klaus Mølmer, Holographic Quantum Computing, Phys. Rev. Lett. **101**, 040501 (2008).

[11] L. Childress, A. S. Sørensen, and M. D. Lukin, Mesoscopic cavity quantum electrodynamics with quantum dots, Phys. Rev. A **69**, 042302 (2004).

[12] Audrey Cottet and Takis Kontos, Spin Quantum Bit with Ferromagnetic Contacts for Circuit QED, Phys. Rev. Lett. **105**, 160502 (2010).

[13] Pei-Qing Jin, Michael Marthaler, Alexander Shnirman, and Gerd Schon, Strong Coupling of Spin Qubits to a Transmission Line Resonator, Phys. Rev. Lett. **108**, 190506 (2012).

[14] P. Zhang, Ze-Liang Xiang, and Franco Nori, Spin-orbit qubit on a multiferroic insulator in a superconducting resonator, Phys. Rev. B **89**, 115417 (2014).

[15] J. Stehlik, Y.-Y. Liu, C. M. Quintana, C. Eichler, T. R. Hartke, and J. R. Petta, Fast Charge Sensing of a Cavity-Coupled Double Quantum Dot Using a Josephson Parametric Amplifier, Phys. Rev. Applied **4**, 014018 (2015).

[16] Atac Imamoğlu, Cavity QED Based on Collective Magnetic Dipole Coupling: Spin Ensembles as Hybrid Two-Level Systems, Phys. Rev. Lett. **102**, 083602 (2009).

[17] J. H. Wesenberg, A. Ardavan, G. A. D. Briggs, J. J. L. Morton, R. J. Schoelkopf, D. I. Schuster, and K. Mølmer, Quantum Computing with an Electron Spin Ensemble, Phys. Rev. Lett. **103**, 070502 (2009).

[18] D. I. Schuster, A. P. Sears, E. Ginossar, L. DiCarlo, L. Frunzio, J. J. L. Morton, H. Wu, G. A. D. Briggs, B. B. Buckley, D. D. Awschalom, and R. J. Schoelkopf, High-Cooperativity Coupling of Electron-Spin Ensembles to Superconducting Cavities, Phys. Rev. Lett. **105**, 140501 (2010).

[19] Y. Kubo, F. R. Ong, P. Bertet, D. Vion, V. Jacques, D. Zheng, A. Dreau, J.-F. Roch, A. Auffeves, F. Jelezko, J. Wrachtrup, M. F. Barthe, P. Bergonzo, and D. Esteve, Strong Coupling of a Spin Ensemble to a Superconducting Resonator, Phys. Rev. Lett. **105**, 140502 (2010).

[20] R. Amsüss, Ch. Koller, T. Nöbauer, S. Putz, S. Rotter, K. Sandner, S. Schneider, M. Schramböck, G. Steinhauser, H. Ritsch, J. Schmiedmayer, and J. Majer, Cavity QED with Magnetically Coupled Collective Spin States, Phys. Rev. Lett. **107**, 060502 (2011).

[21] D. Marcos, M. Wubs, J. M. Taylor, R. Aguado, M. D. Lukin, and A. S. Sørensen, Coupling Nitrogen-Vacancy Centers in Diamond to Superconducting Flux Qubits, Phys. Rev. Lett. **105**, 210501 (2010).

[22] J. Twamley and S. D. Barrett, Superconducting cavity bus for single nitrogen-vacancy defect centers in diamond, Phys. Rev. B **81**, 241202(R) (2010).

[23] P. Rabl, S. J. Kolkowitz, F. H. L. Koppens, J. G. E. Harris, P. Zoller, and M. D. Lukin, A quantum spin transducer based on nanoelectromechanical resonator arrays, Nat. Phys. **6**, 602 (2010).

[24] Brian Julsgaard, Cécile Grezes, Patrice Bertet, and Klaus Mølmer, Quantum Memory for Microwave Photons in an Inhomogeneously Broadened Spin Ensemble, Phys. Rev. Lett. **110**, 250503 (2013).

[25] S. D. Bennett, N. Y. Yao, J. Otterbach, P. Zoller, P. Rabl, and M. D. Lukin, Phonon-Induced Spin-Spin Interactions in Diamond Nanostructures: Application to Spin Squeezing, Phys. Rev. Lett. **110**, 156402 (2013).
[26] S. Carretta, A. Chiesa, F. Troiani, D. Gerace, G. Amoretti, and P. Santini, Quantum Information Processing with Hybrid Spin-Photon Qubit Encoding, Phys. Rev. Lett. **111**, 110501 (2013).
[27] Martin Leijnse and Karsten Flensberg, Coupling Spin Qubits via Superconductors, Phys. Rev. Lett. **111**, 060501 (2013).
[28] Alexey A. Kovalev, Amrit De, and Kirill Shtengel, Spin Transfer of Quantum Information between Majorana Modes and a Resonator, Phys. Rev. Lett. **112**, 106402 (2014).
[29] L. J. Zou, D. Marcos, S. Diehl, S. Putz, J. Schmiedmayer, J. Majer, and P. Rabl, Implementation of the Dicke Lattice Model in Hybrid Quantum System Arrays, Phys. Rev. Lett. **113**, 023603 (2014).
[30] Christopher O'Brien, Nikolai Lauk, Susanne Blum, Giovanna Morigi, and Michael Fleischhauer, Interfacing Superconducting Qubits and Telecom Photons via a Rare-Earth-Doped Crystal, Phys. Rev. Lett. **113**, 063603 (2014).
[31] E. R. MacQuarrie, T. A. Gosavi, N. R. Jungwirth, S. A. Bhave, and G. D. Fuchs, Mechanical Spin Control of Nitrogen-Vacancy Centers in Diamond, Phys. Rev. Lett. **111**, 227602 (2013).
[32] S. D. Bennett, S. Kolkowitz, Q. P. Unterreithmeier, P. Rabl, A. C. Bleszynski Jayich, J. G. E. Harris, and M. D. Lukin, Measuring mechanical motion with a single spin, New J. Phys. **14**, 125004 (2012).
[33] Z. Y. Xu, Y. M. Hu, W. L. Yang, M. Feng, and J. F. Du, Deterministically entangling distant nitrogen-vacancy centers by a nanomechanical cantilever, Phys. Rev. A **80**, 022335 (2009).
[34] Mohamed Almokhtar, Masazumi Fujiwara, Hideaki Takashima, and Shigeki Takeuchi, Numerical simulations of nanodiamond nitrogen-vacancy centers coupled with tapered optical fibers as hybrid quantum nanophotonic devices, Opt. Express **22**, 20045 (2014).
[35] Bo-Bo Wei, Christian Burk, Jörg Wrachtrup, and Ren-Bao Liu, Magnetic ordering of nitrogen-vacancy centers in diamond via resonator-mediated coupling, EPJ Quantum Technology **2**, 18 (2015).
[36] Burm Baek, William H. Rippard, Matthew R. Pufall, Samuel P. Benz, Stephen E. Russek, Horst Rogalla, and Paul D. Dresselhaus, Spin-Transfer Torque Switching in Nanopillar Superconducting-Magnetic Hybrid Josephson Junctions, Phys. Rev. Applied **3**, 011001 (2015).
[37] Y. Kubo, C. Grezes, A. Dewes, T. Umeda, J. Isoya, H. Sumiya, N. Morishita, H. Abe, S. Onoda, T. Ohshima, V. Jacques, A. Dréau, J.-F. Roch, I. Diniz, A. Auffeves, D. Vion, D. Esteve, and P. Bertet, Hybrid Quantum Circuit with a Superconducting Qubit Coupled to a Spin Ensemble, Phys. Rev. Lett. **107**, 220501 (2011).
[38] Y. Tao, J. M. Boss, B. A. Moores, and C. L. Degen, Single-crystal diamond nanomechanical resonators with quality factors exceeding one million, Nat. Commun. **5**, 3638 (2014).
[39] Preeti Ovartchaiyapong, Kenneth W. Lee, Bryan A. Myers, and Ania C. Bleszynski Jayich, Dynamic strain-mediated coupling of a single diamond spin to a mechanical resonator, Nat. Commun. **5**, 4429 (2014).
[40] J. Teissier, A. Barfuss, P. Appel, E. Neu, and P. Maletinsky, Strain Coupling of a Nitrogen-Vacancy Center Spin to a Diamond Mechanical Oscillator, Phys. Rev. Lett. **113**, 020503 (2014).
[41] Patrik Rath, Svetlana Khasminskaya, Christoph Nebel, Christoph Wild, and Wolfram H. P. Pernice, Diamond-integrated optomechanical circuits, Nat. Commun. **4**, 1690 (2013).
[42] Michael J. Burek, Daniel Ramos, Parth Patel, Ian W. Frank, and Marko Loncar, Nanomechanical resonant structures in single-crystal diamond, Appl. Phys. Lett. **103**, 131904 (2013).
[43] P. Ovartchaiyapong, L. M. A. Pascal, B. A. Myers, P. Lauria, and A. C. Bleszynski Jayich, High quality factor single-crystal diamond mechanical resonators, Appl. Phys. Lett. **101**, 163505 (2012).
[44] Behzad Khanaliloo, Harishankar Jayakumar, Aaron C. Hryciw, David P. Lake, Hamidreza Kaviani, and Paul E. Barclay, Diamond nanobeam waveguide optomechanics, arXiv:1502.01788v1.
[45] Marcus W. Doherty, Neil B. Manson, Paul Delaney, Fedor Jelezko, Jörg Wrachtrup, and Lloyd C. L. Hollenberg, The nitrogen-vacancy colour centre in diamond, Phys. Rep. **528**, 1 (2013).
[46] M. Gao, C. W. Wu, Z. J. Deng, W. J. Zou, L. Zhou, C. Z. Li, and X. B. Wang, Controllable strong coupling between individual spin qubits and a transmission line resonator via nanomechanical resonators, Phys. Lett. A **376**, 595 (2012).
[47] C. A. Regal and K. W. Lehnert, From cavity electromechanics to cavity optomechanics, J. Phys. Conf. Ser. **264**, 012025 (2011).
[48] N. Didier and R. Fazio, Putting mechanics into circuit quantum electrodynamics, C.R. Phys. **13**, 470 (2012).
[49] J. D. Teufel, Dale Li, M. S. Allman, K. Cicak, A. J. Sirois, J. D. Whittaker, and R. W. Simmonds, Circuit cavity electromechanics in the strong-coupling regime, Nature (London) **471**, 204 (2011).
[50] Quirin P. Unterreithmeier, Eva M. Weig, and Jörg P. Kotthaus, Universal transduction scheme for nanomechanical systems based on dielectric forces, Nature (London) **458**, 1001 (2009).
[51] P. Rabl, P. Cappellaro, M. V. Gurudev Dutt, L. Jiang, J. R. Maze, and M. D. Lukin, Strong magnetic coupling between an electronic spin qubit and a mechanical resonator, Phys. Rev. B **79**, 041302(R) (2009).
[52] T. Faust, J. Rieger, M. J. Seitner, J. P. Kotthaus, and E. M. Weig, Coherent control of a classical nanomechanical two-level system, Nat. Phys. **9**, 485 (2013).
[53] Simon Rips and Michael J. Hartmann, Quantum Information Processing with Nanomechanical Qubits, Phys. Rev. Lett. **110**, 120503 (2013).
[54] See Appendixes A, B, and C for more details.
[55] J. Venermo and A. Sihvola, Dielectric polarizability of circular cylinder, J. Electrost. **63**, 101 (2005).

[56] T. J. Kippenberg and K. J. Vahala, Cavity optomechanics: Back-action at the mesoscale, Science **321**, 1172 (2008).

[57] F. Marquardt and S. M. Girvin, Optomechanics, Physics **2**, 40 (2009).

[58] I. Wilson-Rae, N. Nooshi, W. Zwerger, and T. J. Kippenberg, Theory of Ground State Cooling of a Mechanical Oscillator Using Dynamical Backaction, Phys. Rev. Lett. **99**, 093901 (2007).

[59] F. Marquardt, J. P. Chen, A. A. Clerk, and S. M. Girvin, Quantum Theory of Cavity-Assisted Sideband Cooling of Mechanical Motion, Phys. Rev. Lett. **99**, 093902 (2007).

[60] Yong-Chun Liu, Yun-Feng Xiao, Xingsheng Luan, and Chee Wei Wong, Dynamic Dissipative Cooling of a Mechanical Resonator in Strong Coupling Optomechanics, Phys. Rev. Lett. **110**, 153606 (2013).

[61] J. D. Teufel, T. Donner, Dale Li, J. W. Harlow, M. S. Allman, K. Cicak, A. J. Sirois, J. D. Whittaker, K. W. Lehnert, and R. W. Simmonds, Sideband cooling of micromechanical motion to the quantum ground state, Nature (London) **475**, 359 (2011).

[62] Jasper Chan, T. P. Mayer Alegre, Amir H. Safavi-Naeini, Jeff T. Hill, Alex Krause, Simon Gröblacher, Markus Aspelmeyer, and Oskar Painter, Laser cooling of a nanomechanical oscillator into its quantum ground state, Nature (London) **478**, 89 (2011).

[63] S. Hong, M. S. Grinolds, P. Maletinsky, R. L. Walsworth, M. D. Lukin, and A. Yacoby, Coherent, mechanical control of a single electronic spin, Nano Lett. **12**, 3920 (2012).

[64] O. Arcizet, V. Jacques, A. Siria, P. Poncharal, P. Vincent, and S. Seidelin, A single nitrogen-vacancy defect coupled to a nanomechanical oscillator, Nat. Phys. **7**, 879 (2011).

[65] Zhang Qi Yin, Tong Cang Li, Xiang Zhang, and L. M. Duan, Large quantum superpositions of a levitated nanodiamond through spin-optomechanical coupling, Phys. Rev. A **88**, 033614 (2013).

[66] G. Balasubramanian, P. Neumann, D. Twitchen, M. Markham, R. Kolesov, N. Mizuochi, J. Isoya, J. Achard, J. Beck, J. Tissler, V. Jacques, P. R. Hemmer, F. Jelezko, and J. Wrachtrup, Ultralong spin coherence time in isotopically engineered diamond, Nat. Mater. **8**, 383 (2009).

[67] K. Bergmann, H. Theuer, and B. W. Shore, Coherent population transfer among quantum states of atoms and molecules, Rev. Mod. Phys. **70**, 1003 (1998).

[68] K. Eckert, M. Lewenstein, R. Corbalán, G. Birkl, W. Ertmer, and J. Mompart, Three-level atom optics via the tunneling interaction, Phys. Rev. A **70**, 023606 (2004).

[69] K. Eckert, J. Mompart, R. Corbalán, M. Lewenstein, and G. Birkl, Three level atom optics in dipole traps and waveguides, Opt. Commun. **264**, 264 (2006).

[70] F. Dreisow, A. Szameit, M. Heinrich, R. Keil, S. Nolte, A. Tünnermann, and S. Longhi, Adiabatic transfer of light via a continuum in optical waveguides, Opt. Lett. **34**, 2405 (2009).

[71] J. R. Johansson, P. N. Nation, and F. Nori, Qutip 2: A python framework for the dynamics of open quantum systems, Comput. Phys. Commun. **184**, 1234 (2013).

[72] W. Weaver, S. P. Timoshenko, and D. H. Young, *Vibration Problems in Engineering*, 5th ed. (Wiley, New York, 1990).

[73] L. D. Landau and E. M. Lifshitz, *Theory of Elasticity* (Butterworth-Heinemann, Oxford, 1986).

[74] R. N. Simons, *Coplanar Waveguide Circuits, Components, and Systems* (Wiley, New York, 2004).

[75] R. N. Simons and R. K. Arora, Coupled slot line field components, IEEE Trans. Microwave Theory Tech. **30**, 1094 (1982).

[76] C. L. Degen, H. J. Mamin, M. Poggio, and D. Rugar, Nuclear magnetic resonance imaging with 90-nm resolution, Nat. Nanotechnol. **2**, 301 (2007).